Renewable Energy 34 (2009) 297–306

Contents lists available at ScienceDirect

Renewable Energy

journal homepage: www.elsevier.com/locate/renene

Steam jet ejector cooling powered by waste or solar heat

A.J. Meyer*, T.M. Harms [1], R.T. Dobson [1]

Department of Mechanical and Mechatronic Engineering, University of Stellenbosch, PO Box x1, Matieland 7602, South Africa

ARTICLE INFO

Article history:
Received 20 November 2006
Accepted 23 March 2008
Available online 15 August 2008

Keywords:
Steam jet ejector
Solar energy
Solar refrigeration
Waste heat

ABSTRACT

A small scale steam jet ejector experimental setup was designed and manufactured. This ejector setup consists of an open loop configuration and the boiler operate in the temperature range of $T_b = 85–140\ ^\circ C$. The typical evaporator liquid temperatures range from $T_e = 5\ ^\circ C$ to $10\ ^\circ C$ while the typical water-cooled condenser pressure ranges from $P_c = 1.70$ kPa to 5.63 kPa ($T_c = 15–35\ ^\circ C$). The boiler is powered by two 4 kW electric elements while a 3 kW electric element simulates the cooling load in the evaporator. The electric elements are controlled by means of variacs.

Primary nozzles with throat diameters of 2.5 mm, 3.0 mm and 3.5 mm are tested while the secondary ejector throat diameter remains unchanged at 18 mm. These primary nozzles allow the boiler to operate in the temperature range of $T_b = 85–110\ ^\circ C$. When the nozzle throat diameter is increased, the minimum boiler temperature decreases. A primary nozzle with a 3.5 mm throat diameter was tested at a boiler temperature of $T_b = 95\ ^\circ C$, an evaporator temperature of $T_e = 10\ ^\circ C$ and a critical condenser pressure of $P_{crit} = 2.67$ kPa (22.6 °C). The system's COP is 0.253.

In a case study the experimental data of a solar powered steam jet ejector air conditioner is investigated. Solar powered steam ejector air conditioning systems are technical and economical viable when compared to conventional vapour compression air conditioners. Such a system can either utilise flat plate or evacuated tube solar thermal collectors depending on the type of solar energy available.

1. Introduction

The aim of this research is to investigate the possibility to run a steam jet ejector on boiler temperatures below 100 °C. If this can be achieved, conventional solar flat plate or evacuated tube water heaters can be used to power a steam jet ejector to produce refrigeration or cooling.

Small scale jet ejectors that operate on a boiler temperatures range of 120–140 °C are well documented in Refs. [1–3]. Steam ejectors that operate at boiler temperatures below 110 °C are, however, not well documented. The aim of this research was to investigate the operation of an ejector at boiler temperatures in the range of $T_b = 95–105\ ^\circ C$.

2. The steam jet cycle

A steam jet refrigerator was first developed by Le Blanc and Parson as early as 1900 [4]. It experienced great popularity during the early 1930s for air conditioning systems of large buildings [5]. The system was replaced with the more favourable vapour compression system. The latter system was superior in its coefficient of performance (COP), flexibility and compactness in manufacturing and operation [6].

The steam ejector cycle is similar to the conventional vapour compression cycle except that the compressor is replaced by a liquid feed pump, boiler and ejector-pump. In brief, liquid refrigerant is vaporised at a high pressure in a boiler and fed to an ejector where it entrains a low pressure vapour originating from the evaporator. This combined flow is then compressed to an intermediate pressure equal to that of the condenser. This cycle has recently drawn renewed attention due to its simplicity of construction, ruggedness and few or no moving parts.

Fig. 1 presents a schematic of the conventional ejector refrigeration cycle. The cycle typically consists of the boiler, the ejector, the condenser and the evaporator.

Referring to Fig. 1, the liquid refrigerant boils in the boiler at a high pressure and temperature due to the application of heat. This high-pressure refrigerant vapour passes through line 1 and enters

Abbreviations: CFC, chlorofluorocarbon; COP, coefficient of performance; HCFCs, hydrochlorofluorocarbons; HFCs, hydrofluorocarbons; ID, inner diameter; NXP, primary nozzle exit position; OD, outer diameter; PVC, polyvinyl chloride; UK, United Kingdom.

* Corresponding author. Tel.: +27 21 808 4376; fax: +27 21 808 4958.
E-mail addresses: meyer@sun.ac.za (A.J. Meyer), tmh@sun.ac.za (T.M. Harms), rtd@sun.ac.za (R.T. Dobson).
URL: http://www.mecheng.sun.ac.za
[1] Tel.: +27 21 808 4376; fax: +27 21 808 4958. www.mecheng.sun.ac.za.

0960-1481/$ – see front matter © 2008 Elsevier Ltd. All rights reserved.
doi:10.1016/j.renene.2008.03.020

Nomenclature

A_T	nozzle area ratio [dimensionless]
A_t	nozzle throat area [m^2]
A_R	ejector throat ration [dimensionless]
C_{sc}	solar collector constant [W/°C m^2]
d	diameter [mm]
G	solar irradiation [W/m^{-2}]
h	specific heat [kJ/kg]
m	mass flow rate [kg/s]
P	pressure/electric power [Pa]/[W]
P_{c^*}	critical condenser pressure [Pa]
Q	heat [J]
R_m	entrainment ratio [dimensionless]
s	entropy [kJ/kg K]
T	temperature [°C]
V	volume [m^3]
W	work [J]

Greek symbols

η	efficiency [%]
ρ	density [kg/m^3]

Subscripts

a	ambient
b	boiler
c, cond	condenser
d	diffuser
e, evap	evaporator
f	fluid
g	gas (vapour)
m	mixing chamber/mean
t	throat

the primary nozzle of the ejector compressor. A typical ejector cross-section with pressure and velocity profiles is shown in Fig. 2. The primary stream accelerates and expands through a convergent–divergent (de Laval) nozzle to produce a supersonic flow (typically Mach number above 2), which creates a low pressure region. This partial vacuum created by the supersonic primary flow entrains refrigerant vapour from the evaporator through momentum transfer in line 2. The evaporator pressure falls and boiling of the refrigerant in the evaporator occurs at a low pressure and consequently at a low temperature.

The primary and secondary streams mix in the mixing chamber and enter a normally choked (sonic flow conditions at the throat) secondary converging–diverging nozzle. The flow expands in the diffuser part of this nozzle through a thermodynamic shock process. This shock wave causes a sudden rise in the static pressure and its location varies with the condenser backpressure. The flow emerges from the shock wave with subsonic velocity and is compressed in the diffuser to the saturation pressure of the condenser.

From the diffuser exit, the mixed flow is fed directly to the condenser through line 3 where it is cooled and condensed. The condensate is returned to the evaporator via an expansion valve in line 6 and to the boiler through a feed pump in line 4. A full description of ejector principles and performance including industrial applications is available [8].

Fig. 3 presents a general thermodynamic analysis for the ejector cycle. Different working fluids can be used in an ejector cycle, e.g. halocarbon compounds such as CFCs, HCFCs and HFCs [10], as well as butane, ammonium and water [11].

Water is by far the most environmentally friendly fluid. Using water as working fluid the evaporator temperature typically varies

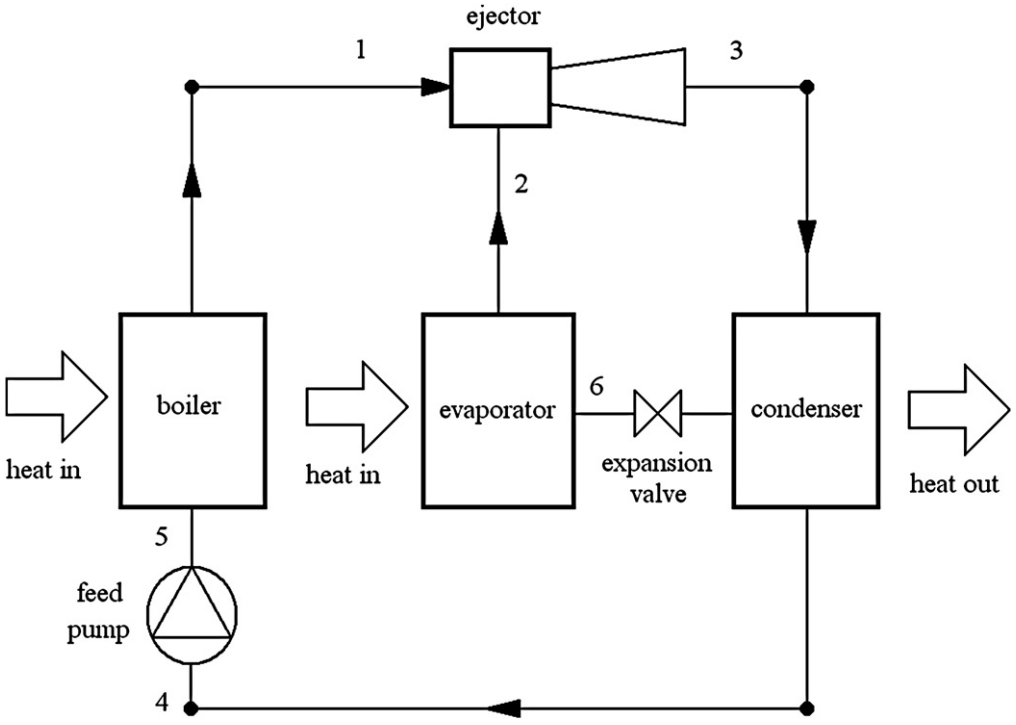

Fig. 1. Ejector cycle.

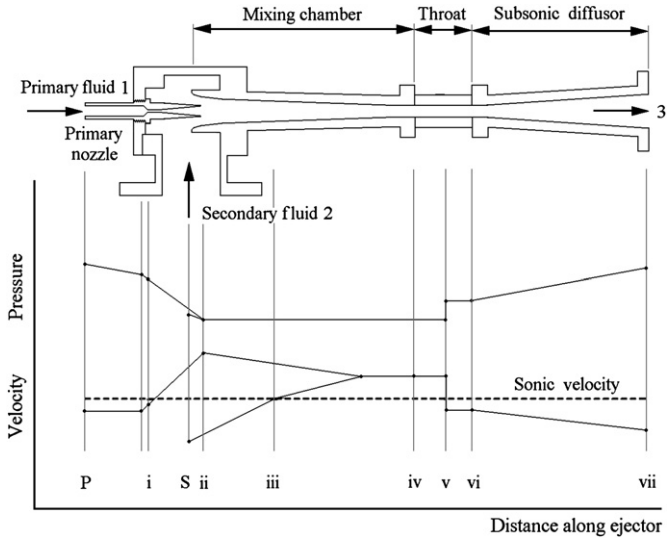

Fig. 2. Typical ejector cross-section and pressure and velocity profiles [redrawn after 7].

in the range 5–15 °C depending on the application. Typical condenser temperatures vary in the range 15–40 °C depending on the condenser type (wet or dry cooled), cooling water temperature and ambient conditions. In practical systems, the boiler temperature should be above 80 °C [2]. COP values for the cycle typically vary in the range of 0.1–0.6 depending on the operating conditions.

3. Description of experimental setup

A photo and accompanying schematic drawing of the experimental setup is included in Figs. 4 and 5, respectively.

The design of the experimental setup was done with the aid of published work [2,10] as well as previous work done at Stellenbosch University [9]. The aim of the design was to keep the system as simple as possible and use off-the-shelf components whenever feasible.

In reference to Figs. 4 and 5 the test facility consists of four principal components: an 8 kW electrical steam boiler (A), a 3 kW evaporator (B), a water-cooled condenser (C) and an ejector assembly (D).

3.1. The boiler (A)

The boiler was manufactured from a 150 mm ID stainless steel pipe 1250 mm in length and 2 mm wall thickness. The bottom and top ends of the pipe were fitted with bolted stainless steel flanges 8 mm in thickness as well as viton o-rings. Two 4 kW electric elements, a thermocouple, two thermostats and a drain valve were mounted on the bottom flange. The top flange is fitted with a variable pressure relief valve, an analogue pressure gauge (F), a steam pipe, a ball valve (E), a thermocouple and a drain valve. The boiler was insulated with 25 mm fibre wool insulation and aluminium cladding was used.

The boiler water level is measured by means of a sight glass. The sight glass was manufactured from a 12 mm OD and 2 mm wall thickness glass tube. The boiler has a total volume of 22.1 l and the useable volume available between the top of the electric elements and the top of the sight glass is 15.2 l. The boiler was designed to operate at $T_b = 80$–140 °C and the corresponding pressure span of $P_b \approx 45$–360 kPa. At the maximum steam flow of 13.5 kg/h (8 kW boiler electric energy input and $T_b = 140$ °C) the boiler can produce steam for more than an hour. Steam leaves the boiler through a 40 mm ID, 2 mm wall thickness pipe and ball valve (E). The boiler was hydrostatically tested up to 400 kPa before it was fitted.

3.2. The evaporator (B)

The evaporator was manufactured from a 150 mm ID stainless steel pipe 600 mm in length and 2 mm wall thickness. The bottom end was welded closed and fitted with a 3 kW electric element and a thermocouple. The top end of the evaporator has bolted stainless

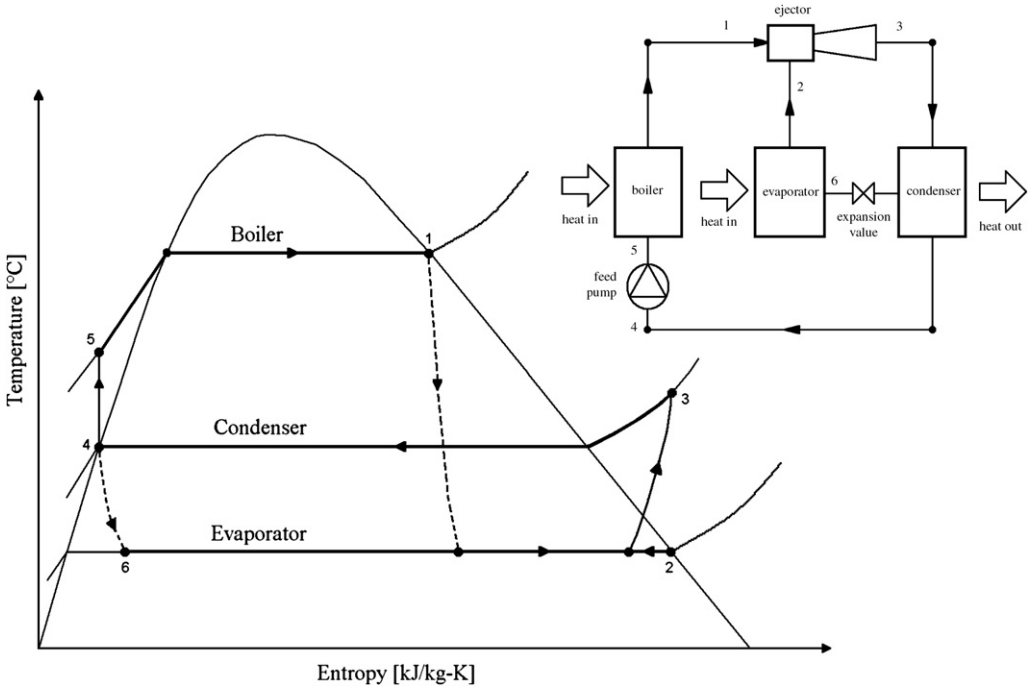

Fig. 3. General steam ejector T–s diagram [redrawn after 9].

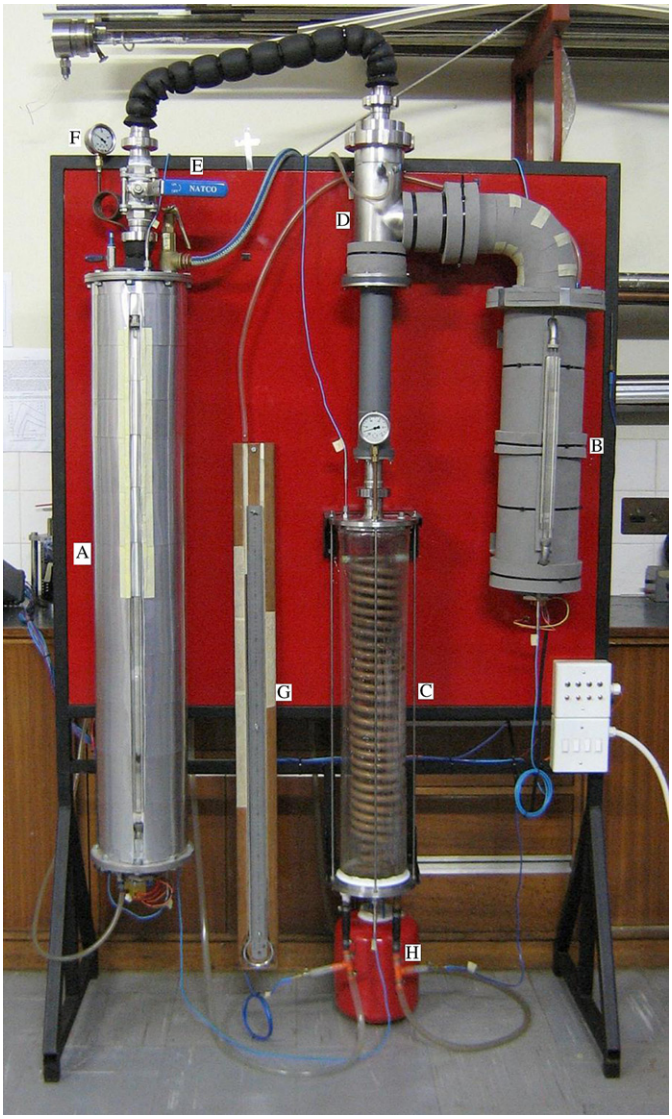

Fig. 4. The ejector experimental setup.

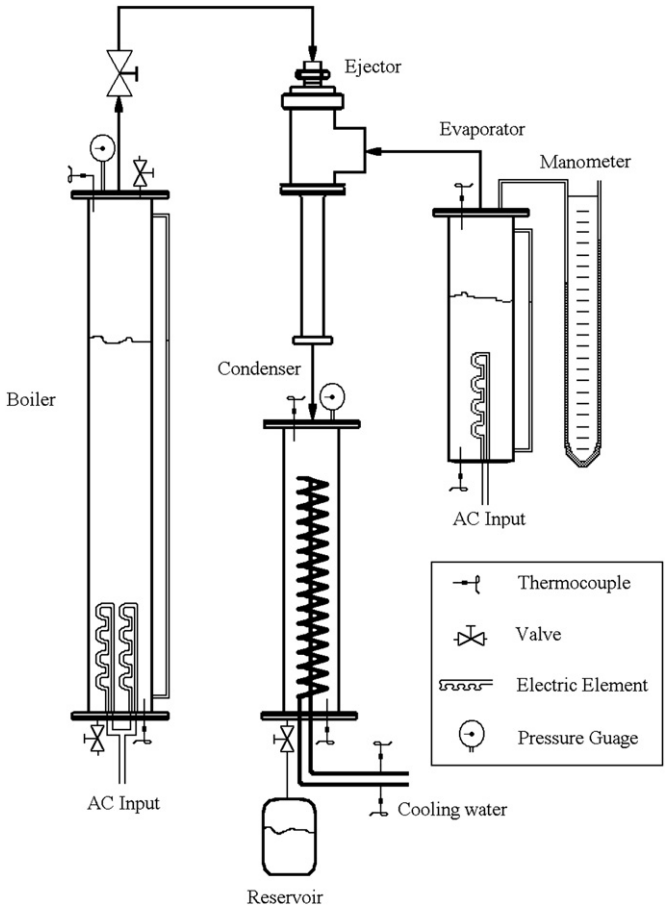

Fig. 5. Schematic of the experimental setup.

steel flanges and an o-ring and is fitted with a thermocouple as well as a mercury manometer (G). The water content is measured with a sight glass similar to that of the boiler. The total volume of the evaporator is 10.6 l and the useable volume between the top of the electric element and the top of the sight glass is 4.1 l.

Water vapour flows from the evaporator to the ejector through a stainless steel pipe and elbow both 100 mm ID. The connection between the evaporator pipe and ejector is done with a 100 mm ID stainless steel union. A connection pipe with a large diameter was chosen due to the high specific volume of steam at low temperatures (147.1 m^3/kg at 5 °C and 77.9 m^3/kg at 15 °C versus 1.67 m^3/kg at 100 °C). A large diameter pipe is necessary to secure a low vapour velocity. With the evaporator operating at maximum electric input of 3 kW and at an evaporator temperature of 5 °C the steam velocity in the 100 mm ID pipe is calculated to be 22.6 m/s.

The evaporator vapour and liquid temperatures are measured with separate thermocouples. The pressure within the evaporator is determined by means of the steam tables as well as with the mercury manometer (G). A difference between these two pressures mentioned indicates the presence of air in the evaporator. The evaporator is insulated with 10 mm thick Armaflex insulation.

The electric element simulates the evaporator cooling load. This element is controlled with a variac.

3.3. The condenser (C)

A boiler unit from a previous experimental setup was modified to be used as a condenser. A 150 mm diameter Perspex pipe 800 mm long and with 3 mm wall thickness is fitted with stainless steel flanges. Silicone was used to secure an airtight joint between the Perspex and endplates. The top plate is fitted with a thermocouple and an analogue pressure gauge. This plate also connects to the bottom of the ejector through a 40 mm stainless steel pipe and union as can be seen in Fig. 4. The bottom plate has a drain valve, thermocouple and a cooling water inlet and outlet.

Inside the condenser is a copper cooling coil. This coil was manufactured from 15 mm OD plain copper pipe and wound in two spirals. The outer spiral has an OD of 120 mm and the inner spiral has an OD of 85 mm. Fifteen metres of copper pipe were used and the wounded coil is approximately 700 mm long.

The temperature inside the condenser is controlled by the cooling water flow rate. The minimum temperature in the condenser is limited by the temperature of the cooling water. The total volume of the condenser is 14.1 l without the cooling coil. The volume of the condenser with the cooling coil fitted is 11.5 l. The cooling water inlet and outlet pipes are both fitted with thermocouples.

A receiver tank (H) with a capacity of 8 l is connected to the outlet of the condenser. This tank serves as a reservoir for the condensate.

3.4. The ejector (D)

The outer body in which the nozzle is situated is made from a standard 100 mm ID, 2 mm wall thickness stainless steel T-piece. Two 100 mm ID unions connect the T-piece to the boiler and the evaporator. A 1/2″ valve is located near the top of the T-piece which is used along with the vacuum pump to remove air from the system.

A flange and o-ring connect the T-piece to the secondary nozzle. The secondary nozzle is manufactured from a solid piece of PVC 150 mm in diameter and 325 mm in length (Fig. 6). This nozzle has a throat length of 40 mm and is 18 mm in diameter. The secondary nozzle throat is a critical dimension in the proper operation of the system. The secondary nozzle profile was obtained from published data [1].

The primary nozzle and spacers are manufactured from brass and viton o-rings are used. The spacers and nozzle screw into a flange that is connected to the T-piece. There are six spacers (40 mm, 45 mm, 50 mm, 60 mm, 70 mm, 80 mm length). By using different combinations of spacers, the nozzle position can vary relative to the flange they screw into with 5 mm intervals. Table 1 lists the dimensions of the different nozzles.

3.5. Other components

A 40 mm ID, 2 mm wall thickness stainless steel pipe connects the boiler and ejector assembly. This pipe is tilted at an angle of 15° with respect to the horizon. Condensate that forms inside this pipe can run back to the boiler (Fig. 4). This pipe is covered with 10 mm thick Armaflex insulation.

A data logger connected to a personal computer is used to log the temperatures from the T-type thermocouples. The voltage to each electric element is also recorded.

Notice that the test facility has no pump between the condenser and boiler and no expansion valve between the condenser and evaporator. Such a system is termed an open loop system.

3.6. The experimental test procedure

Experiments are executed in batches. Before each test run the boiler and evaporator are filled with municipal tap water up to a predetermined level near the top of the sight glass. The boiler valve is closed and air is evacuated from the boiler by using a water-jet vacuum pump connected to the top of the boiler. The next step is to switch the boiler electric elements on.

While the boiler heats up to its operating temperature, the vacuum pump is used to evacuate air from the rest of the system. Notice that the steam pipe, ejector assembly, evaporator and condenser are all connected to each other without any valves. The vacuum pump is connected to the top of the ejector T-piece. When the boiler is at its operating temperature the boiler valve is opened. This allows the connection pipe between the boiler and ejector to be heated. It also serves to drives out the air still trapped in the connection pipe. The boiler valve is only opened for about 5 s at a time. The boiler valve is opened and closed for a few times while the vacuum pump is running. This is done until the air is removed from the connection pipe and the rest of the system.

Next, the boiler valve is closed and the boiler water level is refilled to the predetermined level. The boiler is reheated to its operating temperature. The cooling water to the condenser is turned on and the data logger is switched on. To start a test run, the boiler valve is opened. An immediate rise in condenser pressure is observed while the evaporator temperature falls rapidly. The boiler and evaporator temperatures are controlled with a variac. The thermostat on each boiler element acts as an over-temperature and thus an over-pressure protection. The boiler and evaporator mass flow rate is determined by measuring the total amount of liquid that was converted into steam over the entire time interval of the test run.

4. Results and discussions

4.1. Ejector performance

The thermodynamic performance of a steam ejector is evaluated by the coefficient of performance (COP). This is the ratio of the evaporator heat load and the sum of the boiler energy input and pump work. The COP is calculated as follows:

$$\mathrm{COP} = \frac{\dot{Q}_{\mathrm{evap}}}{\dot{Q}_{\mathrm{boiler}} + \dot{W}_{\mathrm{pump}}} \approx \frac{\dot{Q}_{\mathrm{evap}}}{\dot{Q}_{\mathrm{boiler}}} \tag{1}$$

The pump work can be omitted since it is typically less than 1% of the boiler heat input [1].

For a closed loop cycle, the COP can also be calculated as

$$\mathrm{COP} = R_{\mathrm{m}} \frac{h_{\mathrm{g-evap}} - h_{\mathrm{f-cond}}}{h_{\mathrm{g-boiler}} - h_{\mathrm{f-cond}}} \tag{2}$$

where R_{m} represents the entrainment ratio defined as

$$R_{\mathrm{m}} = \frac{\dot{m}_{\mathrm{e}}}{\dot{m}_{\mathrm{b}}} \tag{3}$$

For an open loop cycle, as described in this paper, the COP can be calculated as

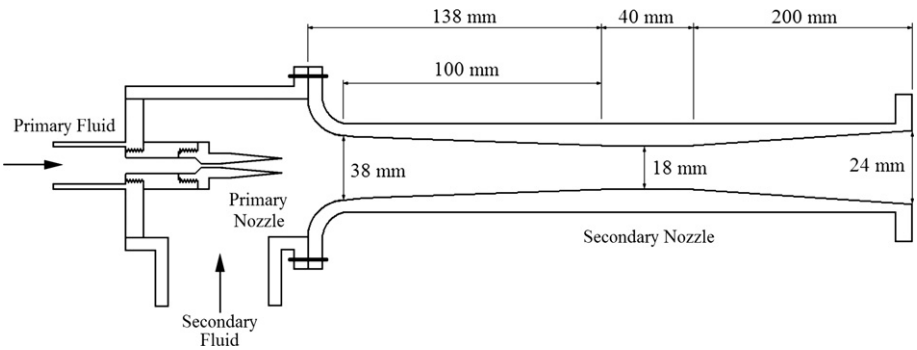

Fig. 6. Secondary nozzle profile.

Table 1
Primary nozzle geometries

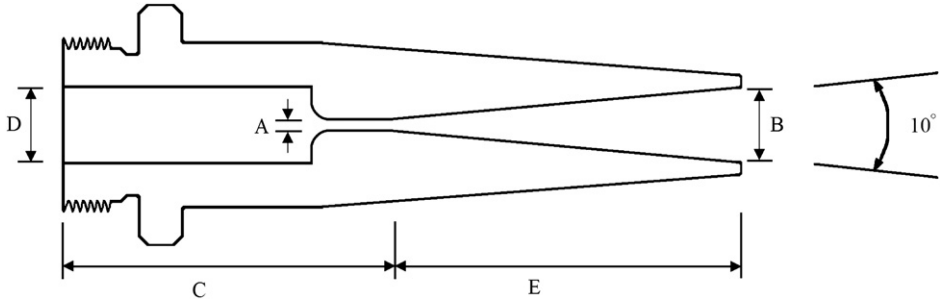

Nozzle number	Geometries [mm]						
	A	B	C	D	E	A_T[a]	A_R[b]
1	1.5	6	69.25	8	25.75	16	144.0
2	1.75	7	65	8	30	16	105.8
3	2	8	60.7	8	34.3	16	81.0
4	2.5	8	60.7	8	34.3	16	51.8
5	2.5	10	42.85	8	52.15	16	51.8
6	3	12	51.5	8	43.5	16	36.0
7	3.5	14	60	8	35	16	26.4

$d_{t\text{-secondary}} = 18.0$ mm.
[a] $A_T = \text{Area}_B/\text{Area}_A$.
[b] $A_R = A_{t\text{-secondary}}/A_{t\text{-primary}}$.

$$\text{COP} = R_m \frac{h_{g-evap} - h_{f-evap}}{h_{g-boiler} - h_{f-boiler}} \quad (4)$$

From Eqs. 2 and 4 it can be expected that the open loop COP would be higher than the closed loop COP. This is mainly due to the additional heat energy required in the closed loop system to heat up the condensate returned to the boiler to the boiler temperature. For a boiler temperature of $T_b = 100$ °C, a condenser temperature of $T_c = 25$ °C and an evaporator temperature of $T_e = 10$ °C, the ratio of an open loop COP to a closed loop COP is 1.168.

4.2. Boiler temperature and primary nozzle throat diameter

No published data on primary nozzle throat diameters and ejector profiles could be found for experimental systems that operate below 110 °C. In order to find the nozzle throat diameter that corresponds to an optimum boiler temperatures in the range $T_b = 95$–105 °C and evaporator temperatures of $T_e = 10$ °C, primary nozzles with different throat sizes were tested for a constant secondary nozzle throat diameter of 18 mm. Since a 2 mm diameter primary nozzle operated at a $T_b = 130$ °C, primary nozzles with throat diameters of 2.5 mm, 3.0 mm and 3.5 mm were tested. The results of these experiments are included in Fig. 7. The specifications of each nozzle are listed in Table 1.

It can be observed from Fig. 7 that an optimum COP can be achieved at a 90 °C boiler temperature using primary nozzle 7. The reduced boiler temperature is at the expense of the COP. During the experiment, the condenser pressure was not allowed to drop below 2.0 kPa (18.3 °C). As the boiler temperature decreases, the critical condenser pressure increases correspondingly. The reason for the sudden drop in COP as the boiler temperature decreases is due to the critical condenser pressure that falls below the threshold value of 2.0 kPa.

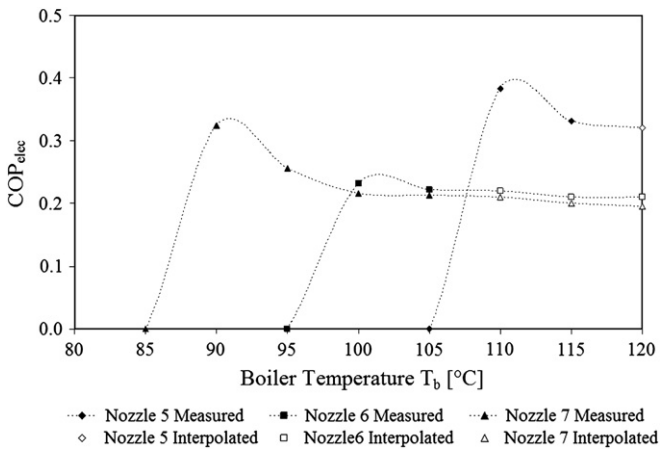

Fig. 7. COP versus boiler temperature for different primary nozzles ($P_c \geq 2.0$ kPa, $T_c \geq 18.3$ °C, $T_e = 10$ °C, NXP = −5 mm).

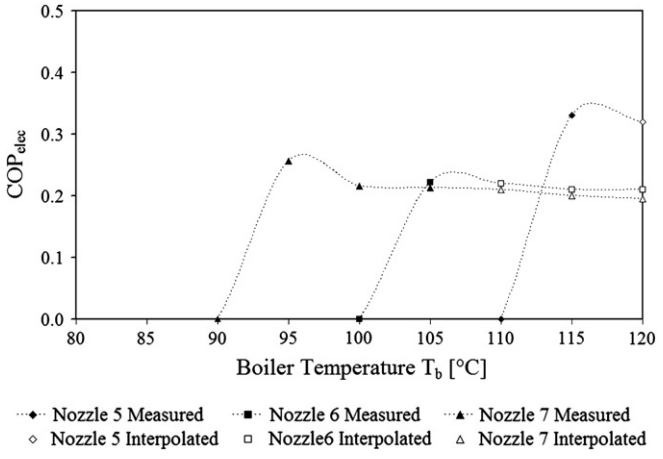

Fig. 8. COP versus boiler temperature for different primary nozzles ($P_c \geq 2.34$ kPa, $T_c \geq 20$ °C, $T_e = 10$ °C, NXP = −5 mm).

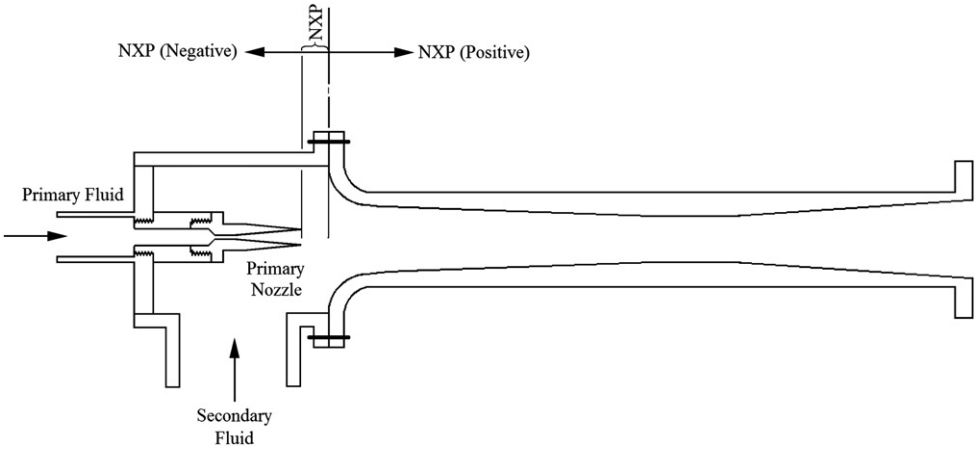

Fig. 9. Primary nozzle exit position.

In an additional experiment, P_c was limited to 2.34 kPa (20 °C). The result of increasing the condenser threshold pressure is an increase of the optimum boiler temperature and a decrease in COP (Fig. 8). It is therefore advantageous to have a condenser pressure as low as possible.

4.3. Primary nozzle exit position

The primary nozzle exit position (NXP) is defined as the distance from the primary nozzle exit to the bell-mouth inlet of the mixing chamber. NXP is measured in mm and is positive when the primary nozzle exit is down-stream of the mixing chamber inlet (Fig. 9).

The effect of the primary nozzle position on the system performance is given in Figs. 10 and 11. It is clear from Fig. 10 that NXP = −5 mm is the optimum operating point for nozzle 7. If the primary nozzle is too far upstream from the bell-mouth inlet, the COP drops. In a similar manner, the COP drops if NXP is too large (primary nozzle inside the secondary nozzle).

4.4. Comparing experimental results and the theoretical model

The theoretical model published by Eames et al. [6] was entered into an Excel spread sheet. The theoretical model is used to predict a critical condenser pressure by using the boiler and evaporator temperatures as well as entrainment ratio values.

In this paper, three different theoretical models are used. Each model has different values for the primary nozzle efficiency η_p, the diffuser efficiency η_d and the mixing chamber efficiency η_m. The efficiency values for "theory one" are $\eta_p = 0.85$, $\eta_d = 0.85$ and $\eta_m = 0.95$ as suggested by Eames et al. [6]. The values for "theory two" are $\eta_p = 0.8$, $\eta_d = 0.8$ and $\eta_m = 0.8$ and for "theory three" they are $\eta_p = 0.75$, $\eta_d = 0.75$ and $\eta_m = 0.75$.

The effect of η_d is relatively small on the critical condenser pressure. A 10% change in η_d only has a 0.2% effect on P_c. η_m has the largest influence on P_c. A 10% change in η_m changes P_c by 14.1%. A 10% change in η_p has a 3.4% effect on P_c. It is clear from this information that the mixing efficiency between the primary and secondary streams η_m dominates the performance of the ejector.

In Fig. 12 a comparison is presented between the experimental results of Eames et al. [10] and the three theoretical models.

The experimental results of Eames et al. [10] show that the COP is on average 60% lower than the entrainment value. This difference is due to the unwanted heat losses from the boiler and heat gains to the evaporator from the environment. The entrainment ratio compares well to theory one and on average only differ by 3.5%.

Since the theory does not make provision for the primary nozzle exit position, the best COP values obtained for nozzle 7 were used to compare to the theory. The best COP results were obtained at NXP = −5 mm. Nozzle 7 with $T_e = 10$ °C and $T_b = 95$–105 °C was compared to the three different theory scenarios in Fig. 13.

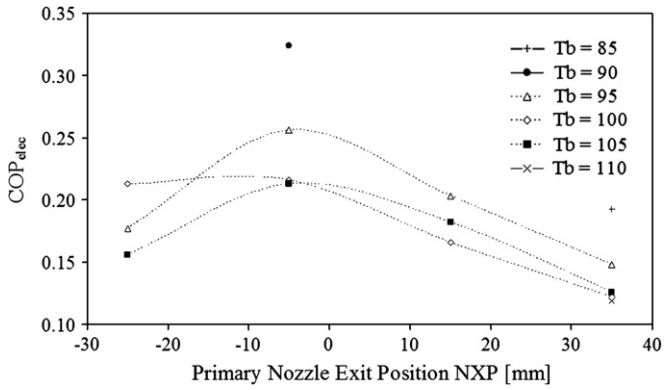

Fig. 10. The effect of primary nozzle exit position on system performance for nozzle 7.

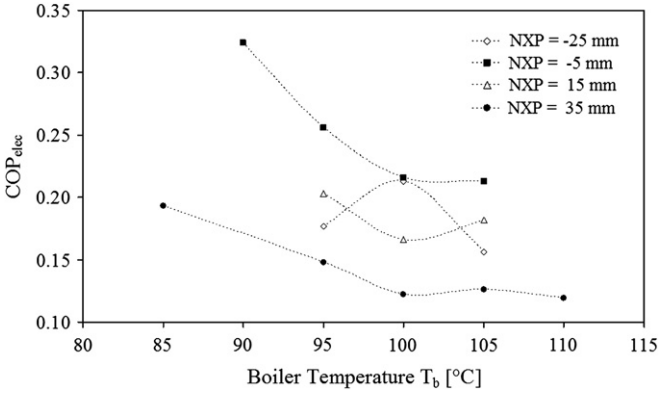

Fig. 11. The effect of primary nozzle exit position on system performance for nozzle 7.

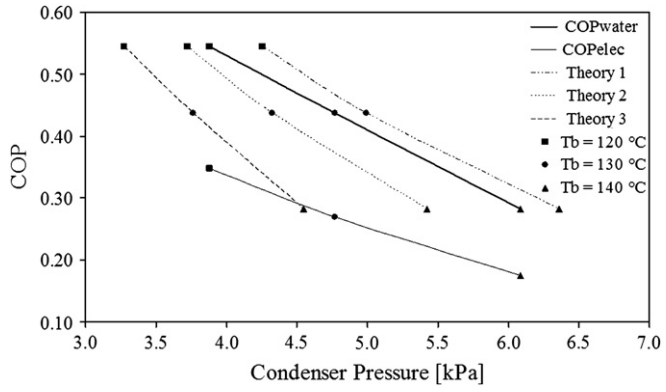

Fig. 12. COP and entrainment ratio compared to three theoretical models: $T_e = 10$ °C, $A_R = 81$, and NXP = 26 mm [10].

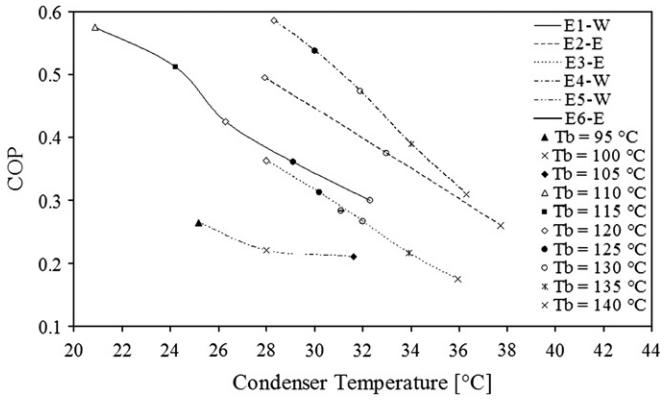

Fig. 14. Comparison of different published data for $T_b = 95$–140 °C and $T_c = 10$ °C.

As expected and can be seen from Fig. 13, the COP and entrainment ratio differs. The COP differs in the range of 85.3–99.1% in comparison with the entrainment ratio. This value is considerably higher than the value recorded by Eames et al. [10] of 60%. The main reasons for this could be that the apparatus used in this thesis was reasonably well insulated and was operated at lower boiler temperatures.

The experimental COP values compare the best with theoretical model three. The entrainment ratio compares on average within 39.4% with comparison to theoretical model one, within 14.8% with comparison to theoretical model two and within 10.4% with comparison to theoretical model three.

The apparatus used by Eames et al. [10] used a water circulation pump and spray nozzle system in the evaporator. The lack of such a system in the apparatus that was tested could be the reason for the large deviation from theoretical model one. Another reason could be the lower boiler to condenser pressure ratio at which the tests were conducted which can lead to higher inefficiencies that will reduce the system performance.

4.5. Comparison to published data

Fig. 14 and Table 2 present the experimental results of various authors. These differ due to the differences in equipment, primary nozzle exit position and area ratios. Note that E2, E3 and E6 represent COP values and E1, E4 and E5 represent entrainment ratios.

The purpose of this comparison is to form a general idea of work done until present on steam jet ejectors. From Fig. 14, it could be concluded that higher COP and lower T_{crit} values would be expected from the experiments. The A_R value for E5, however, is significant lower than E1–E4.

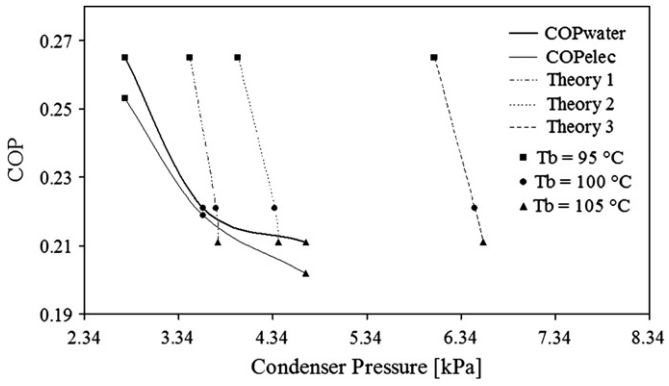

Fig. 13. COP and entrainment ratio compared to three theoretical models: $T_b = 95$–105 °C, $T_e = 10$ °C, and $A_R = 26.5$.

5. Solar energy

5.1. General

The use of solar energy for the boiler of a jet ejector system is not a novel idea and can be tracked back to the 1960s [12,13]. Various articles have been published suggesting different working fluids for a solar powered ejector refrigerator, e.g. R113 [14], R134a [15,16], R141b [17,18], ammonia [19], water, methanol and ethanol [20]. It can be noticed from the dates of these articles that there is a renewed focus worldwide into solar powered ejector refrigeration and cooling.

5.2. Solar collectors

The type of solar radiation (percentage of direct and diffused sunlight) of each location would determine the type of solar collector that can be used. Evacuated tube collectors are the superior choice compared to flat plate solar collectors in terms of diffused solar radiation conditions. The operating temperatures of these collectors are listed in Table 3.

In a study, Huang et al. [23] compared three different solar collectors as listed in Table 4.

The efficiency of each collector is given by

$$\eta_{sc} = 0.8 - C_{sc}\frac{T_m - T_a}{G} \quad (6.1)$$

where T_m is the mean fluid temperature in the panel [°C], T_a is the ambient temperature [°C], G is the solar irradiance [W/m^2], and C_{sc} is the collector constant [W/°C m^2] (Refer to Table 4).

Table 2
Comparison of different published data

Data series	Author[a]	Measured data	System	A_R	NXP [mm]	T_e [°C]
E1	1	R_m	Closed	81	–	10
E2	2	COP	Closed	90	26.16	10
E3	3	COP	Closed	81	26	10
E4	4	R_m	Closed	90	26.16	10
E5	5	R_m	Open	36	16	10
E6	6	COP	Open	81	25	10

[a] (1) Sun (1996) [27], (2) Chunnanond and Aphornratana [3,7], (3) Aphornratana and Eames [1], (4) Eames et al. [6,10], (5) author – nozzle 7, and (6) author – nozzle 3.

Table 3
Typical operating temperatures of different solar collectors [21,22]

Type of collector	Typical operating temperature
Flat plate collector	<70
High efficiency flat plate collector	60–120
Evacuated tube collector	60–130

According to Fig. 15, the evacuated tube collectors are more efficient than flat plate solar collectors. Flat plate collectors, however, are less expensive compared to evacuated tube collectors. Other advantages of flat plate collectors are ease of installation, durability and they can be produced locally with simple tools. This makes flat plate collectors more attractive for developing countries. The disadvantage of flat plate collectors is that they take up more space than evacuated tube collectors. Currently no concentrating collectors, including evacuated tube collectors, are commercially produced in South Africa.

5.3. Economic viability of solar powered ejector systems

Nguyen et al. [24] compared their solar powered steam ejector cooling system to a conventional vapour compression air conditioner. The systems were compared over a period of 30 years, which are the expected lifetime of a typical ejector cooling system. The lifetime of a vapour compression system is estimated at 15 years. The required start up capital calculations was based on a bank loan at an annual interest rate of 6%. A 600-h per year running time is assumed. It is further assumed that the ejector system has no maintenance cost while two services per year are required for the vapour compression system.

These authors concluded that, over the 30 years comparison time, the ejector cooling system is slightly more expensive than the vapour compression system. The payback period for an ejector cooling system is approximately 33 years.

A similar economic analysis was performed as part of a proposed solar powered ejector air conditioner for a hospital in Mexico. The system would have a boiler temperature of 160 °C, a condenser temperature of 30 °C and an evaporator temperature of 10 °C. The system would have a 13 kW cooling capacity. Due to the high boiler temperatures the COP is predicted to be 0.62. The economic analysis predicted a payback period of 5 years [25,26].

In conclusion, the two case studies represented indicate that a solar driven steam jet ejector air conditioning is economic feasible. In general, the viability of a solar powered ejector air conditioner does depend on the location where the system is installed which in turn determines the available sunlight, electricity cost and equipment prices.

6. Conclusions

A working prototype of a steam jet ejector was manufactured and successfully operated at boiler temperatures below 100 °C.

Table 4
Three different solar collectors [23]

Collector type	Description	C_{sc} [W/°C m^2]
A	Low-cost specially designed single-glazed flat plate collector with a selective surface	3.5
B	A conventional single-glazed solar collector with a selective surface	5.7
C	A vacuum-tube solar collector with tube-in-sheet fin	2

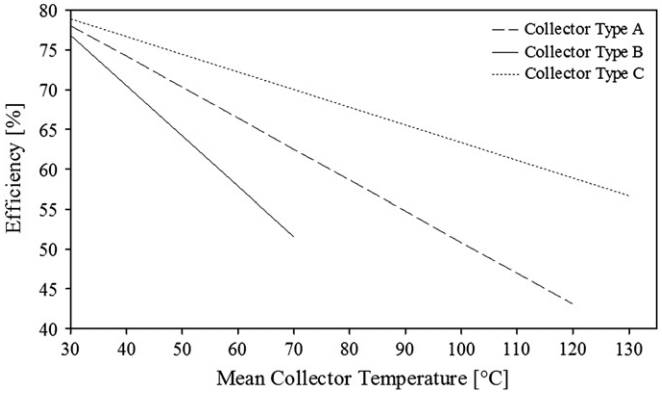

Fig. 15. Efficiency comparison of three types of solar collectors with $T_{ambient} = 25$ °C and $G = 900$ W/m^2.

From the work presented, it can be concluded that the steam jet ejector is a practical viable system at boiler temperatures below 100 °C.

The theoretical model described accounted for the efficiencies of the primary nozzle, mixing chamber and diffuser. Out of these three efficiencies, the diffuser efficiency has the smallest contribution to the system performance. The efficiency of the mixing chamber is more dominant than the efficiencies of the primary nozzle and diffuser. The theory lacks in defining the effect of variations in the primary nozzle exit position.

From the experiments conducted, it can be concluded that the parameters that govern the functioning of a steam jet ejector are boiler temperature, evaporator temperature, critical condenser pressure, primary nozzle exit position and the primary and secondary nozzle throat ratio A_R. A condenser pressure above the critical condenser pressure and the super heating of the primary steam has a negligible or no effect on the system's operation.

Although ample work is published on solar powered ejectors with various working fluids, very few data could be found on solar powered steam ejectors. It is concluded from the case study that was presented that solar powered steam jet air conditioning is practical and economically viable when compared to conventional vapour compression air conditioners.

The next step in the research would be to investigate the performance of a closed loop system at similar boiler temperatures and methods to produce the system economically.

Acknowledgements

The authors would like to thank the South African National Research Foundation who partially funded the project as well as to the Department of Mechanical and Mechatronic Engineering for the availability of their laboratories.

References

[1] Aphornratana S, Eames IW. A small capacity steam-ejector refrigerator: experimental investigation of a system using ejector with movable primary nozzle. International Journal of Refrigeration 1997;20(5):352–8.
[2] Eames IW, Wu S, Worall M, Aphornratana S. An experimental investigation of steam ejectors for application in jet-pump refrigerators powered by low-grade heat. Proceedings of the I MECH E Part A Journal of Power and Energy 1 October 1999;213(5):351–61.
[3] Chunnanond K, Aphornratana S. An experimental investigation of a steam ejector refrigerator: the analysis of the pressure profile along the ejector. Applied Thermal Engineering 2004;24:311–22.
[4] Steam-jet refrigeration equipment, ASHRAE guide and data book. US: ASHRAE; 1969 [chapter 13].
[5] Stoecker WF. Refrigeration and air conditioning. New York: McGraw-Hill; 1959.

[6] Eames IW, Aphornratana S, Haider H. A theoretical and experimental study of a small-scale steam jet refrigerator. International Journal of Refrigeration 1995;18(6):378–86.
[7] Chunnanond K, Aphornratana S. Ejectors: applications in refrigeration technology. Renewable and Sustainable Energy Reviews 2004;8:129–55.
[8] ESDU – Engineering Sciences Data Unit. Ejector and jet pump design for steam driven flow. 251-259 Regent Street, London: Engineering Sciences Data Unit; 1986. Item No. 86030.
[9] Van Wyk PA. Cooling agricultural produce using a vapour-jet ejector. Final year thesis, Department of Mechanical Engineering, University of Stellenbosch, Stellenbosch, South Africa; 2000.
[10] Eames IW, Aphornratana S, Sun DW. The jet-pump cycle-a low cost refrigerator option powered by waste heat. Heat Recovery Systems & CHP 1995;15(8):711–21.
[11] Pridasawas W. Solar-driven ejector refrigeration system. Stockholm, Sweden: Division of Applied Thermodynamics and Refrigeration, Department of Energy Technology, Royal Institute of Technology; 2003.
[12] Çengel YA, Boles MA. Thermodynamics – an engineering approach. 4th ed. McGraw-Hill; 2002 [chapter 16].
[13] Kakabaev A, Davletov A. A Freon ejector solar cooler. Geliotekhnika 1966;2(5):42–8.
[14] Al-Khalidy N. An experimental study of an ejector cycle refrigeration machine operating on R113. International Journal of Refrigeration 1998;21(8):617–25.
[15] Alexis GK, Karayiannis EK. A solar ejector cooling system using refrigerant R134a in the Athens area. Renewable Energy 2005;30:1457–69.
[16] Selvaraju A, Mani A. Experimental investigation on R134a vapour ejector refrigeration system. International Journal of Refrigeration. Available from: <www.sciencedirect.com> 2006.
[17] Huang BJ, Chang JM, Petrenko VA, Zhuk KB. A solar ejector cooling system using refrigerant R141b. Solar Energy 1998;64(4–6):223–6.
[18] Vidal H, Colle S, dos Santos Pereira G. Modelling and hourly simulation of a solar ejector cooling system. Applied Thermal Engineering 2006;26:663–72.
[19] Sankarlal T, Mani A. Experimental studies on an ammonia ejector refrigeration system. International Communications in Heat and Mass Transfer 2006;33:224–30.
[20] Riffat SB, Holt A. A novel heat pipe/ejector cooler. Applied Thermal Engineering 1998;18(3–4):93–101.
[21] Rona N. Solar air-conditioning systems – focus on components and their working principles. Göteborg, Sweden 5765: eBook-edition, Building Services Engineering, Department of Building Technology, Chalmers University of Technology; 2004. Internserie: I2004:01; ISSN: 1652-6007.
[22] Assilzadeh F, Kalogiroub SA, Alia Y, Sopiana K. Simulation and optimization of a LiBr solar absorption cooling system with evacuated tube collectors. Renewable Energy 2005;30:1143–59.
[23] Huang BJ, Petrenko VA, Samofatov IY, Shchetinina NA. Collector selection for solar ejector cooling system. Solar Energy 2001;7(4):269–74.
[24] Nguyen VN, Riffat SB, Doherty PS. Development of a solar-powered passive ejector cooling system. Applied Thermal Engineering 2001;21:157–68.
[25] Wolpert JL, Nguyen MV, Riffat SB. Hybrid solar/gas cooling ejector unit for a hospital in Mexico. Institute of Building Technology, School of the Built Environment; University of Nottingham; University Park, Nottingham, NG7 2RD. ISES website: <wire0.ises.org/wire/doclibs/SWC1999.nsf/id/793B72DDE2-B79A75C1256920003D618F/$File/109.pdf>; November 2000.
[26] Wolpert JL, Riffat SB, Redshaw S. Prototype for a novel solar powered ejector air conditioning system in Mazunte Mexico. In: Proceeding of the international solar energy congress 2003. Gothenburg: University of Nottingham, Institute of Building Technology, Nottingham, United Kingdom; 2003.
[27] Sun D. Variable geometry ejectors and their applications in ejector refrigeration systems. Journal of Energy 1996;21(10):919–29.